THE JOURNAL OF PHYSICAL CHEMISTRY C LETTERS

Published on Web 07/21/2007

Anomalous Quasihydrostaticity and Enhanced Structural Stability of 3 nm Nanoceria

Zhongwu Wang*

CHESS, Wilson Laboratory, Cornell University, Ithaca, New York 14853

Sudipta Seal and Swanand Patil

Advanced Materials Processing and Analysis center, Mechanical, Materials, and Aerospace Engineering, Nanoscience and Technology Center, University of Central Florida, 4000 Central Florida Boulevard, Orlando, Florida 32816

Changsheng Zha

Geophysical Laboratory, Carnegie Institution of Washington, Washington, DC 20015

Qing Xue

Intel Corporation, Chandler, Arizona 85226

Received: June 23, 2007; In Final Form: July 11, 2007

High-pressure ruby fluorescence spectroscopy and synchrotron X-ray diffraction are used to investigate the differential stress development and structural stability of 3 nm ceria. Upon compression of nanoceria to ~28.2 GPa, R_1 and R_2 lines of ruby remain consistent in shape and sharpness. X-ray diffraction displays no reasonable evidence of peak broadening to 28.6 GPa and phase transformation to 65.1 GPa. These observations suggest an anomalous quasihydrostatic state of compressed nanoceria and a highly enhanced structural stability. Although a pressure-driven oxygen release and subsequent vacancy-induced interface superfluid reasonably explains the generation of extended quasihydrostaticity, a particle size dependent isotropic stress field and surface energy contribution to total energy explain a reversal of structural stability as compared to the size-induced reduction of transformation pressure in large scale nanoceria. These findings provide significant information not only for understanding the reversed Hall−Petch relation of nanomaterials but also for synthesizing engineering materials with tunable mechanical properties.

Ceria (CeO_2) has been extensively investigated as a catalyst and a promising candidate for solid oxide fuel cells.[1] In this capacity, the formation and transport of oxygen vacancies are pivotal. One effective approach is the particle size tuning. Studies indicate that reducing particle size not only increases oxygen vacancies and surface area for improvement of catalyst efficiency[2] but also changes structural, electronic, and lattice vibrational properties for development of advanced materials.[3~8] Most of these properties display an apparent variation while particle size reduces down to ~10 nm or smaller. Such a critical size has also been observed in a large body of materials.[9] On the contrary to ceria, these materials mostly display size-tuned lattice shrinkage and decreased defect ratio or defect-free. Dynamic simulations of nanomaterials demonstrate that a direct particle-to-particle contact under pressure drives particle and hosted defect to react with others through grain boundary and interface.[10] Below the critical size of ~10 nm, this type of reaction enhances and plays a critical role in tuning of materials properties and performances, especially mechanical properties, such as hardness, toughness, etc.[11] One of the most striking discoveries is the reversal of the well-known Hall−Patch relation upon reduction of particle size down to a critical size. Nanoceria displays an unusual lattice expansion and large oxygen vacancy ratio, so it is expected that a distinct mechanical response comes from ultrafine nanoceria (e.g., <10 nm). As a result, we conducted an in situ high pressure study of 3 nm ceria and explored the particle-to-particle interactions and resulting properties by using diamond anvil cell (DAC) along with in situ optical spectroscopy and synchrotron X-ray diffraction. In this letter, we report an anomalous/extended quasihydrostatic state in compressed ceria without any pressure medium and a reversal of structural stability in which the transition pressure as a function of particle size develops from an initial reduction (30 GPa in bulk vs 23 GPa in 10 nm ceria) to a significant enhancement (>65.1 GPa in 3 nm ceria). A size-dependent stress field and vacancy-involved reaction through interface were employed to decipher the resulting mechanism.

Nanoceria was synthesized using a microemulsion process with cerium nitrate as a precursor and ammonium hydroxide as a coprecipitanting agent.[7] X-ray and electron diffractions indicate that as-synthesized ceria has a cubic fluorite structure ($Fm\bar{3}m$). High-resolution transmission electron microscopy

* Corresponding author. E-mail: zw42@cornell.edu. Tel: 607-255-3551. Fax: 607-255-9001.

10.1021/jp074909g CCC: $37.00

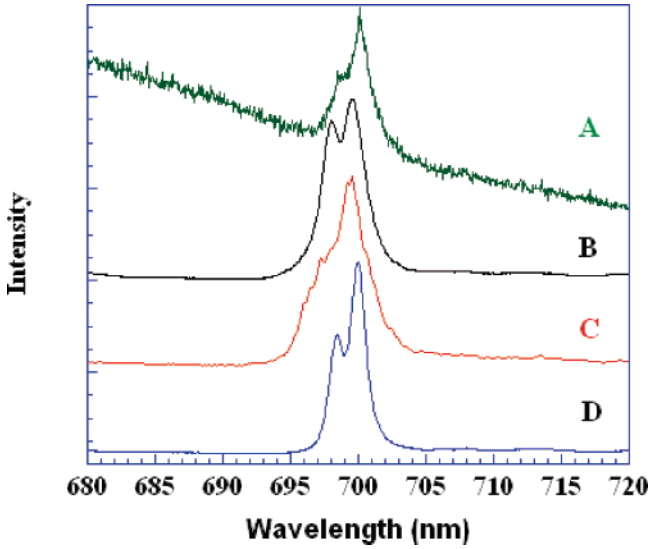

Figure 1. Ruby fluorescence spectra of several samples in different pressure mediums at a close range of pressure. (A) SiC nanocrystals without pressure medium at 16.2 GPa; (B) bulk SiC in a liquid of methanol, ethanol and water at 14.7 GPa; (C) bulk ceria without medium at 15.1 GPa; and D, 3 nm ceria without pressure medium at 15.8 GPa.

(HRTEM) characterizes that ceria has a particle size of 3 nm on average.[7] The samples were loaded in a DAC without a pressure medium, allowing direct particle-to-particle contact for potential interaction. Several ruby chips serve as pressure markers to monitor the pressure gradient and stress distribution across the sample chamber. High-pressure ruby fluorescence spectra were collected by an optical system in which a green laser with a wavelength of 532 nm was used to illuminate the ruby chip. The excited emission signals were collected by a thermoelectrically cooled CCD detector. An in situ pressure energy dispersive synchrotron X-ray diffraction study was conducted at CHESS, Cornell. Energy calibration was made by the well-known radiation sources of ^{55}Fe and ^{133}Ba, whereas angle calibrations were made at $2\theta = 15°$ by the five Bragg diffraction lines of the Au standard.[12] The collected synchrotron X-ray diffraction patterns were used for characterization of crystal structure, differential stress, and particle size.

Ruby displays two strong laser-excited fluorescence peaks: R_1 and R_2. These emission lines are distinct spectroscopically and are very sharp at ambient or hydrostatic pressure conditions. Compression of a material generates deviatoric stress that can be monitored by the shape changes of R_1 and R_2. Upon increasing the magnitude of deviatoric stress, R_1 and R_2 broaden, overlap and eventually merge into a single peak. Ceria is a highly incompressible ceramic, and has a bulk modulus of ~230 GPa.[12] A slight compression of bulk CeO_2 in DAC produces noticeable deviatoric stress and pressure gradient. Figure 1 shows the laser-excited ruby fluorescence spectra of several samples in different pressure mediums at a close range of pressure. At ~15.1 GPa, a pressure gradient across 100 microns of bulk ceria was observed as large as 3~4 GPa, producing an apparent overlapping of R_1 and R_2 (Figure 1C). Similar results were observed in a wide range of nanocrystals as well (e.g., SiC, Figure 1A). Surprisingly, compression of 3 nm ceria did not modify the peak features of R_1 and R_2 (Figure 1D); the shape and sharpness remained almost the same as these observed in bulk materials (e.g., SiC) that were merged in a liquid with a volumetric ratio of methanol/ethanol/water (MEW) = 4:1:1 (Figure 1B). Such a liquid is capable of maintaining a hydrostatic state of a solid to ~12 GPa; above 12 GPa, a quasihydrostatic state is developed. Figure 2 shows

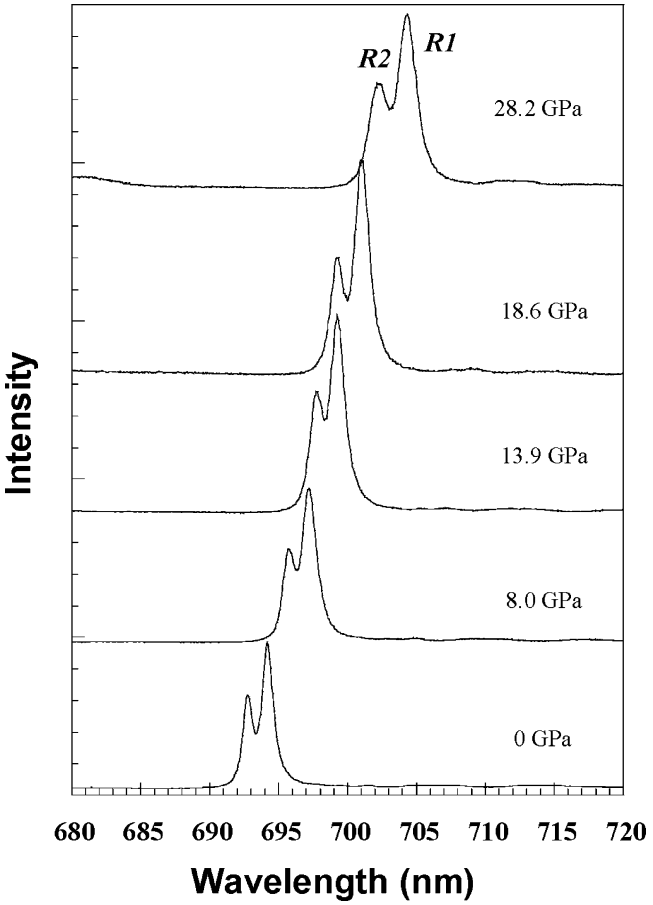

Figure 2. High-pressure ruby fluorescence spectra in 3 nm ceria to a pressure of 28.2 GPa.

that the peak features of ruby in nanoceria remain consistent to pressure as high as 28.2 GPa, indicative of a quasi-hydrostatic state in highly compressed nanoceria.

Energy dispersive synchrotron X-ray diffraction was performed to evaluate the pressure-induced stress field and structural stability of nanoceria. Broadening of the X-ray diffraction peak relates to two factors: particle size and deviatoric stress (differential strain). This can be quantified by the full width at half maximum (fwhm) of X-ray diffraction peaks as a function of pressure. High-pressure X-ray diffraction patterns may differ in intensity and background relatively from one to another because of the variations of beam intensity, time-of-flight, and focusing spot, etc., but these instrumental factors do not contribute a significant influence on the fwhm of X-ray peaks. Without a phase transformation, the pressure-induced reduction of particle size of highly incompressive materials can be ignored within a moderate pressure of 30 GPa due to a slight volumetric shrinkage. Therefore, if particles neither break nor grow, and also hold an isotropic stress field, the fwhm of X-ray peaks during compression should remain identical. Figure 3 shows the key X-ray diffraction patterns of nanoceria at a medium-free environment, indicating that the X-ray peak fwhm remains indistinguishable to pressures as high as 28.6 GPa. Additionally, the inset in Figure 3 reveals that particle size of nanoceria does not change before and after compression to 36.1 and 65.1 GPa. Thus, it is reasonably suggested that a self-driven isotropic stress field results in such a consistency of the fwhm of X-ray diffraction peaks to 28.6 GPa, in agreement with the ruby fluorescence observations and resulting conclusion.

Figure 3 also demonstrates that the cubic fluorite structure of 3 nm ceria is stable to the maximum achieved pressure of

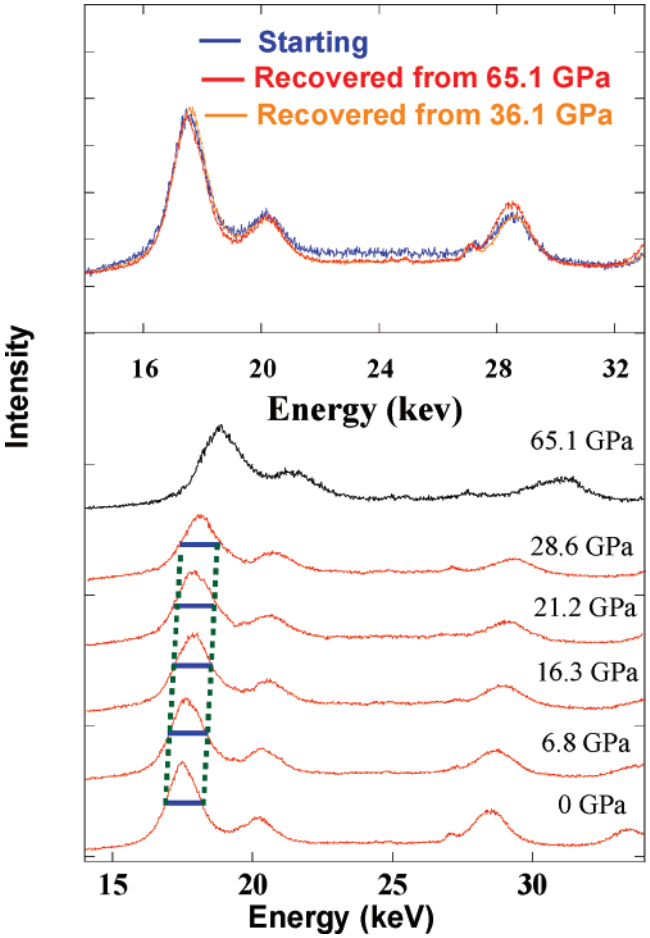

Figure 3. High-pressure X-ray diffraction patterns (XRD) of 3 nm ceria. Inset figure shows a comparison of XRD patterns of starting and recovered ceria. Note: the nonlinear dependence of X-ray intensity on energy and pressure-induced thinning of the samples result in a significant weakening of X-ray diffraction peaks and intensity variation at different energies.

65.1 GPa. High-pressure studies indicate that ceria with a particle size of 10 nm on average transforms to an orthorhombic phase at a lower pressure of ~23 GPa as compared to the transition pressure of ~32 GPa observed in bulk.[12] Obviously, 3 nm ceria does not follow the size-tuned reduction tendency of structural stability predicted from the studies of large scale nanoceria (e.g., >10 nm)[12] and controversially displays a remarkable enhancement. An extended quasihydrostatic state could result in an increase of transition pressure as compared to that in a nonhydrostatic condition, but the resulting difference is only within several gigapascals. Therefore, such a tremendous enhancement with a magnitude of difference as large as ~33 GPa is apparently not induced only by a quasihydrostatic state. It must be related to the specific internal structure of these ultrafine nanoceria.

Extensive studies document that nanoceria displays a significant lattice expansion and a higher oxygen vacancy ratio (Figure 4). These structural properties enhance obviously while particle size reduces down to ~10 nm.[3~8] Deshpande et al. have investigated the oxygen vacancy characteristics of 3 nm ceria,[7] indicative of a vacancy ratio of 0.017 (Figure 4). The lattice parameter is calculated as 5.48 Å, greater than the bulk value of 5.40 Å (inset, Figure 4), indicative of a 4.5% volumetric expansion relative to bulk ceria. These observations agree with the developing trends of vacancy and volumetric expansion as a function of particle size (Figure 4). Previous simulations of

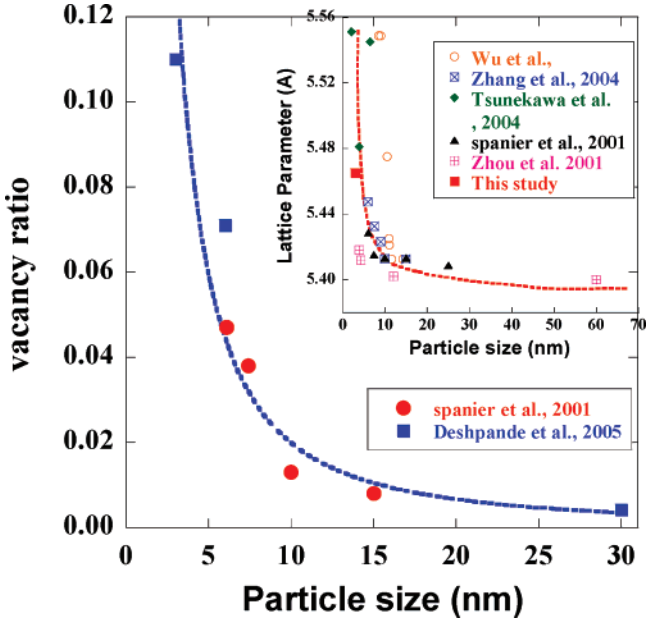

Figure 4. Size-dependent lattice parameter and oxygen vacancy ratio of ceria (Data from refs 3−8 and this study).

nanoceria nucleation indicate that oxygen vacancies prefer to form at the particle surface.[1c] The existence of oxygen vacancy effectively weakens the lattice energy and expands the lattice volume. Compression of ceria induces a stress concentration at oxygen vacancy site. Thermodynamically, a new structural phase prefers to nucleate at a defect or dislocation site from the parent phase, suggesting that oxygen vacancies in ceria serve as a series of nucleation sites to form a new phase. In a perfect crystal, only when pressure approaches a theoretical (maximum) value, it overcomes the energy barrier to form a high-pressure phase, but in a defected ceria, even at a lower pressure, the vacancy-induced stress concentration is capable of driving the formation of a high-pressure phase. This mechanism explains well the size-induced softening of transition pressure as observed in large scale nanoceria but give no answer for the tuning up of the structural stability upon the continuous decrease of particle size. Moreover, the resulting large stress inhomogeneousity in highly defected ceria makes it impossible to explain the observed quasihydrostaticity in 3 nm ceria.

In order to understand the anomalous/extended quasihydrostaticity in compressed ultrafine ceria, two factors need to be considered. As is well-known, ceria is capable of releasing or absorbing oxygen by a reaction of $Ce^{4+} + O^{2-} \leftrightarrow Ce^{3+} + V_O + O_2$, where V_O is oxygen vacancy, and the processing direction depends on its existing environment.[1,2,13] Application of pressure most likely leads to a release of oxygen from nanoceria to fill into the small gap between ceria particles. Therefore, oxygen can serve as a gas pressure medium and produce a hydrostatic state around ceria. Another factor is the existence of a vacancy-induced superfluid state. Solid helium displays a superfluid behavior while cooling to a temperature of 230 mK.[14] Surface defect and boundary instability play critical roles for the formation of a superfluid; application of pressure enhances such a critical effect in these quantum crystals.[15,16] First-principles simulations of solid hydrogen predict that a low-temperature liquid metallic state emerges at a pressure of ~400 GPa, associated with superconducting properties and a rapid kink of melting temperature.[17] A reduction of melting temperature proves to be one striking phenomenon of nanomaterials. When the empirical equation given by Goldstein et al. is applied,[18]

the melting temperature of 3 nm nanoceria can be calculated and is several hundred degrees lower than that of the bulk. Experimental measurements indicate that nanoceria has an enhanced electrical conductivity.[19] Combining these salient properties of nanoceria with the tuning factors and associated properties of a superfluid in solid helium at low temperature and in solid hydrogen under extreme pressure, it is anticipated that a superfluid will appear in nanoceria under compression, thus creating a quasihydrostatic state.

The enhancement of structural stability is closely related to the stress distribution of each single defected particle. Nanomechanic simulations of nanolayer materials under compression indicate that a homogeneous stress field distributes across the entire layer while the nanolayer reduces in thickness down to a critical value. It is most striking that, below this thickness, defects or vacancies do not behave like that in bulk enabling inducing a stress concentration.[20] This thickness can be calculated by $D = (\pi\gamma G)/(h^2)$, where D, γ, G, and h denote critical size (nm), surface energy (J/m^2), Young's modulus (GPa), and Vickers hardness (GPa), respectively. The critical thickness in ceria is therefore predicted to be 7∼18 nm. Nanoceria particles could be assumed as an irregular thin layer in which the largest thickness equals the diameter of the particle. The particle size of ceria in this study is only 3 nm, far below the critical value, attesting that a homogeneous stress distribution field can be generated in each single defected ceria particle upon compression. Therefore, only when pressure is achieved as the same as the transition pressure occurring in a defect-free single crystal, the phase transformation can take place in these ultrafine nanoceria. Meanwhile, the surface energy contribution to the total internal energy has been proved to significantly affect the structural stability, resulting in an apparent increase of transition pressure, particularly for ultrafine particles.[21] Therefore, a combination of particle-related stress field and surface energy contribution can reasonably explain the remarkable enhancement of the transition pressure in 3 nm ceria, rather than a continuous reduction of transition pressure observed in large scale defected nanoceria (e.g., >10 nm). This mechanism can also be applied to explain the reversal of mechanical properties (e.g., reversed Hall−Petch relation) of nanomaterials. It is quite useful for tuning up the yield strength and toughness of hard materials and composites for practical applications.

In summary, high-pressure ruby fluorescence spectroscopy and synchrotron X-ray diffraction studies have been conducted to explore the particle-to-particle interaction of 3 nm ceria and the resulting stress distribution and structural stability. Results indicate the generation of an anomalous/extended quasihydrostatic state within highly compressed nanoceria and remarkable enhancement of structural stability relative to bulk and size-induced reduction of transition pressure in large scale nanoceria. A quasihydrostatic state remains to a pressure as high as 28.6 GPa; the structural stability extends at least to 65.1 GPa. Although a pressure-driven release of oxygen and vacancy-induced surface superfluid at interface can explain the extended quasihydrostaticity, the size-dependent isotropic stress field and surface energy contribution explain the enhanced structural stability. These results not only cast significant implication for understanding the reversal of the Hall−Petch relation through a large body of nanomaterials but also have important application for synthesizing novel engineering materials with tunable mechanical properties.

Acknowledgment. CHESS is supported by the National Science Foundation and NIH-NIGMS via NSF Grant DMR-0225180. We appreciate technical assistances from CHESS staff members. Special thanks go to Darren Dale, Quan Hao, and Sol Gruner at Cornell University for critical reading and comments.

References and Notes

(1) (a) Steele, B. C. H. *Nature (London)* **2001**, *414*, 345. (b) Feng, X.; Sayle, D. C.; Wang, Z. L.; Paras, M. S.; Santora, B.; Sutorik, A. C.; Sayle, T. X. T.; Yang, Y.; Ding, Y.; Wang, X. D.; Her, Y. S. *Science* **2006**, *312*, 1504. (c) Sayle, T. X. T.; Parker, S. C.; Sayle, D. C. *Phys. Chem. Chem. Phys.* **2005**, *7*, 2936.

(2) Tschope, A.; Schaadt, D.; Birringer, R.; Ying, J. Y. *Nanostruct. Mater.* **1997**, *9*, 423.

(3) Zhou, X. D.; Huebner, W. *Appl. Phys. Lett.* **2001**, *79*, 3512.

(4) Tsunekawa, S.; Ito, S.; Kawazoe, Y. *Appl. Phys. Lett.* **2004**, *85*, 3845.

(5) Wu, L.; Wiesmann, H. J.; Moodenbaugh, A. R.; Klie, R. F.; Zhu, Y.; Welch, D. O.; Suenaga, M. *Phys. Rev. B* **2004**, *69*, 125415.

(6) Zhang, F.; Jin, Q.; Chan, S. W. *J. Appl. Phys.* **2004**, *95*, 4319.

(7) Deshpande, S.; Patil, P.; Kuchibhatla, S. V.; Seal, S. *Appl. Phys. Lett.* **2005**, *87*, 133113.

(8) Spanier, J. E.; Robinson, R. D.; Zhang, F.; Chan, S. W.; Herman, I. P. *Phys. Rev. B* **2001**, *46*, 245407.

(9) Meyer, M. A.; Mishra, A.; Benson, D. J. *Prog. Mater. Sci.* **2006**, *51*, 427.

(10) Schiotz, J.; Jacobsen, K. W. *Science* **2003**, *301*, 1357.

(11) Yip, S. *Nat. Mater.* **2004**, *3*, 11.

(12) Wang, Z. W.; Saxena, S. K.; Pischedda, V.; Liermann, H. P.; Zha, C. S. *Phys. Rev. B* **2001**, *64*, 012102.

(13) Conesa, J. C. *Surf. Sci.* **1995**, *339*, 337.

(14) Kim, E.; Chan, M. H. W. *Science* **2004**, *305*, 1941.

(15) Sasaki, S.; Ishiguro, R.; Caupin, F.; Maris, H. J.; Balibar, S. *Science* **2005**, *313*, 1098.

(16) Ceperley, D. *Nat. Phys.* **2006**, *2*, 659.

(17) Babaev, E.; Sudbo, A.; Ashcroft, N. W. *Phys. Rev. Lett.* **2005**, *95*, 105301.

(18) Goldstein, A. N.; Echer, C. M.; Alivisatos, A. P. *Science* **1992**, *256*, 1425.

(19) Tschope, A.; Sommer, E.; Birringer, R. *Solid State Ionics* **2001**, *139*, 255.

(20) Gao, H.; Ji, B.; Jager, I. J.; Arzt, E.; Fratzle, P. *Proc. Natl. Acad. Sci.* **2003**, *110*, 5597.

(21) Tolbert, S. H.; Alivisatos, A. P. *J. Chem. Phys.* **1995**, *102*, 4642.